THE JOURNAL OF PHYSICAL CHEMISTRY B
A JOURNAL OF THE AMERICAN CHEMICAL SOCIETY

pubs.acs.org/JPCB

Article

Stealthy Player in Lipid Experiments? EDTA Binding to Phosphatidylcholine Membranes Probed by Simulations and Monolayer Experiments

Katarina Vazdar,[⊥] Carmelo Tempra,[⊥] Agnieszka Olżyńska, Denys Biriukov, Lukasz Cwiklik,* and Mario Vazdar*

Cite This: *J. Phys. Chem. B* 2023, 127, 5462−5469

Read Online

ACCESS | Metrics & More | Article Recommendations | Supporting Information

ABSTRACT: Ethylenediaminetetraacetic acid (EDTA) is frequently used in lipid experiments to remove redundant ions, such as Ca^{2+}, from the sample solution. In this work, combining molecular dynamics (MD) simulations and Langmuir monolayer experiments, we show that on top of the expected Ca^{2+} depletion, EDTA anions themselves bind to phosphatidylcholine (PC) monolayers. This binding, originating from EDTA interaction with choline groups of PC lipids, leads to the adsorption of EDTA anions at the monolayer surface and concentration-dependent changes in surface pressure as measured by monolayer experiments and explained by MD simulations. This surprising observation emphasizes that lipid experiments carried out using EDTA-containing solutions, especially of high concentrations, must be interpreted very carefully due to potential interfering interactions of EDTA with lipids and other biomolecules involved in the experiment, e.g., cationic peptides, that may alter membrane-binding affinities of studied compounds.

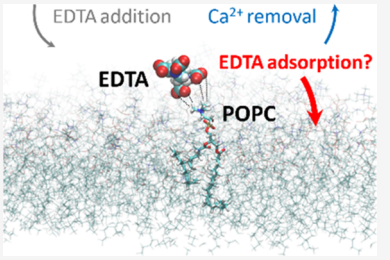

INTRODUCTION

Ethylenediaminetetraacetic acid (EDTA) is a long-used synthetic aminopolycarboxylic acid prepared for the first time in 1935 and mainly known for its metal-chelating properties.[1−3] It is effectively utilized for the complexation of several multivalent cations but most frequently is applied for forming water-soluble complexes with iron (both Fe^{2+} and Fe^{3+})[4,5] and calcium Ca^{2+} ions at neutral pH in solution.[6] Due to its versatile metal-chelating properties,[7] it has found a staggering number of applications in industry, medicine, and household. EDTA is used for treating mercury and lead poisoning,[8] as a preservative in different drug formulations,[9,10] the food industry,[11] and in the cosmetic industry for stabilization of formulations during air exposure.[12] Additionally, EDTA as well as other metal chelators are known to induce permeabilization of the outer membrane in Gram-negative bacteria.[13] It is speculated that EDTA actively removes metal ions from the bacterial membrane, resulting in the loss of lipopolysaccharides and proteins, leading to cell lysis.[14] On the fun side, due to all of the listed various EDTA applications in academic and commercial applications, "strong additional evidence of the efficient use" of EDTA has also been reported in popular culture.[15]

In academic research, EDTA has an invaluable position as an efficient metal chelator for removing redundant ions in solution[16] and biological membranes[17] or inhibiting metal-dependent proteins.[18,19] As such, it is almost always used as an additive in the preparation of a whole range of buffers in biological and biophysical investigations on cells and liposomal cell models, with the aim of total removal of leftover Ca^{2+} ions in Milli-Q water (which are inevitably present in the low nM concentration in our experimental conditions) as well as its sequestration from the biological membranes where they easily bind.[20] Surprisingly, there are very few studies that aimed to test whether EDTA itself binds to lipids and what could be possible consequences of such interaction. For instance, EDTA was noted to have an enhancing effect on the action activity of antiglaucoma drugs by increasing the permeability of the corneal membrane.[21] Galla et al. have reported the fluidization and expansion effect of EDTA in higher concentrations on the phase behavior of dipalmitoylphosphatidylcholine (DPPC) monolayers, brought upon by the electrostatic interaction of negatively charged carboxylic groups of EDTA with the positively charged headgroup of DPPC.[22] Using AFM, they have shown that intercalation of EDTA in the DPPC monolayer induces a membrane curvature, whose size and magnitude depend on the length of exposure to EDTA. However, the molecular picture of the interaction has been only qualitatively described using simple molecular mechanics and semiempirical PM3 calculations on solvent-free models,

Received: May 15, 2023
Revised: May 29, 2023
Published: June 12, 2023

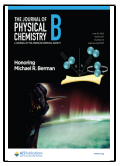

https://doi.org/10.1021/acs.jpcb.3c03207
J. Phys. Chem. B 2023, 127, 5462−5469

thereby entirely disregarding the dynamical component of the interaction, which might be relevant for the described membrane curvature changes.[22] Essentially, to the best of our knowledge, EDTA action on membranes has not been carefully considered yet at the molecular level, and its sequestration of Ca^{2+} ions from lipid membranes is very often taken for granted without a sufficient understanding of whether the addition of EDTA to biological samples has any other effect on corresponding experiments. Considering that only a minimal concentration of Ca^{2+} is always present in Milli-Q water (in a low nM concentration range) while EDTA is added in much higher mM concentration to lipid systems (ranging from 0.1 mM[23,24] to even 5 mM in some buffers used in cell biological experiments for membrane protein extraction[25,26]), an obvious possible interaction of the significant excess of EDTA anions with lipid membranes leading to their adsorption and consequent implications has surprisingly never been studied. In this work, we tackle this open question and systematically investigate the adsorption of EDTA anions (whose distribution depending on the pH of the solution is shown in Figure 1) to 1-palmitoyl-2-oleoylphosphatidylcholine

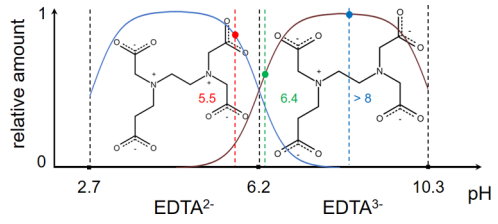

Figure 1. Relative amount of $EDTA^{2-}$ (blue line) and $EDTA^{3-}$ (brown line) in water according to the Henderson–Hasselbach equation[27] as a function of corresponding EDTA pK_a values. For low 50 nM EDTA experiments, the measured pH of the solution is 5.5, and EDTA is present as $EDTA^{2-}$ in ca. 80% and $EDTA^{3-}$ ca. 20% (red dot). At 50 μM EDTA concentration, pH is 6.4, and the amount of $EDTA^{2-}$ and $EDTA^{3-}$ is similar (green dot). At higher EDTA concentrations (1, 3, 15, and 150 mM), the measured pH values are slightly larger than 8, and almost all EDTA ions in the solution are in the $EDTA^{3-}$ form (blue dot).

(POPC) monolayers as the simplest model of lipid membranes combining the custom Langmuir-trough monolayer experiments with computer simulations.

METHODS

Simulation Details. The initial POPC monolayer structure was taken from the publicly available data on the Zenodo server (DOI: 10.5281/zenodo.838633).[28] This structure contains a slab of water placed in the center of the box and two POPC monolayers (256 lipids each) located at the interfaces with a ~12 nm thick vacuum (Figure S1). This system was used to prepare all other simulation setups by adding ions, including EDTA in different protonation forms. The complete composition of the simulated systems is summarized in Table S1. The obtained systems were energy minimized, and then 1 μs long production runs were carried out. The first 100 ns were considered as equilibration and disregarded from the analysis. All simulations were run using an NVT ensemble with an area per lipid of POPC of roughly 70 $Å^2$ (0.70 nm^2). The force field used for POPC and ions is CHARMM36,[29] while water was modeled using the four-point OPC model.[30] This combination of force fields was selected based on the recent work discussing the accuracy of lipid monolayer simulations.[31] The model for EDTA anions was built using the Ligand Reader & Modeler module[32] in CHARMM-GUI[33] (Figure S2), and corresponding atom types and partial charges derived using CGenFF[34] are given in Table S2. The equation of motion was solved using a 2 fs timestep and leap-frog algorithm, with an updating frequency of 20 steps. The smooth particle mesh Ewald with a cutoff of 1.2 nm was used to treat electrostatic interactions.[35] Van der Waals interactions were treated using a cutoff of 1.2 nm, with the forces smoothly attenuated to zero between 1.0 and 1.2 nm. The dispersion correction to energy and pressure was applied to account for long-range Lennard–Jones interactions.[36] The temperature was maintained constant at 298 K using a Nose–Hoover thermostat with three coupling groups (POPC, EDTA anions, and remaining ionic aqueous solution). All covalent bonds involving hydrogens were constrained using the P-LINCS algorithm.[37] All simulations were performed using Gromacs, versions 2021 and 2022.[38]

Experimental Details. Measurements of monolayer surface pressure kinetics (adsorption kinetics) were performed with an in-house built microwell (round shape interface of 7 cm^2, 5 mL subphase volume, perforation present for injection of solutions directly into subphase). The system was equipped either with an ultrasensitive surface pressure sensor (Kibron) with the DyneProbe or NIMA surface tensiometer. 15 μL of 0.1 mM solution of POPC (purchased from Avanti Polar Lipids, Alabaster, AL) in chloroform was spread by deposition of small droplets with a Hamilton microsyringe over 4 mL of Milli-Q water (Millipore, 18.2 MΩ·cm, pH 5.5, the concentration of Ca^{2+} was in low nM range) to achieve a surface pressure of 20 mN m^{-1}. The surface pressure change was monitored for 30 min needed for chloroform evaporation and monolayer stabilization. Once the surface pressure of the POPC monolayer stabilized, EDTA and $CaCl_2$ in appropriate amounts (corresponding to concentrations of 50 nM, 50 μM, and 3 mM of EDTA, and 50 μM EDTA + 50 μM $CaCl_2$, respectively) were administered using the Hamilton microsyringe to the subphase below the monolayer, and the pressure was monitored for further 30 min. Measurements were performed at room temperature. To slow down subphase evaporation and protect the film from dust and additional disruptions, an acrylic cover box over the setup was used.

Langmuir monolayer surface pressure–molecular area (π–A) compression isotherms were measured with a commercially available MicroTrough setup (59 mm × 209 mm) (μtrough XS, Kibron; Helsinki, Finland). The system was equipped with an ultrasensitive surface pressure sensor (KBN 315; Kibron) with the DyneProbe. 12.5 μL of 1 mM solution of POPC in chloroform was spread by deposition of small droplets with a Hamilton microsyringe over 25 mL of Milli-Q water or solutions of EDTA of corresponding concentrations. The π–A isotherms were collected during the symmetrical movement of two barriers controlled by software (FilmWare) provided by the equipment manufacturer. The compression speed was 10 mm/min (i.e., 3.92 $Å^2$/chain/min for the POPC monolayer). Measurements were done at 25.0 °C, controlled with a temperature control plate (connected to a water-circulating thermostat; ±0.5 °C accuracy) placed under the trough. To slow down subphase evaporation and protect from dust and additional surface disruptions, an acrylic cover box over the trough was used. Before each measurement, the lipid film was left uncovered for 3 min to allow chloroform to evaporate and

https://doi.org/10.1021/acs.jpcb.3c03207
J. Phys. Chem. B 2023, 127, 5462–5469

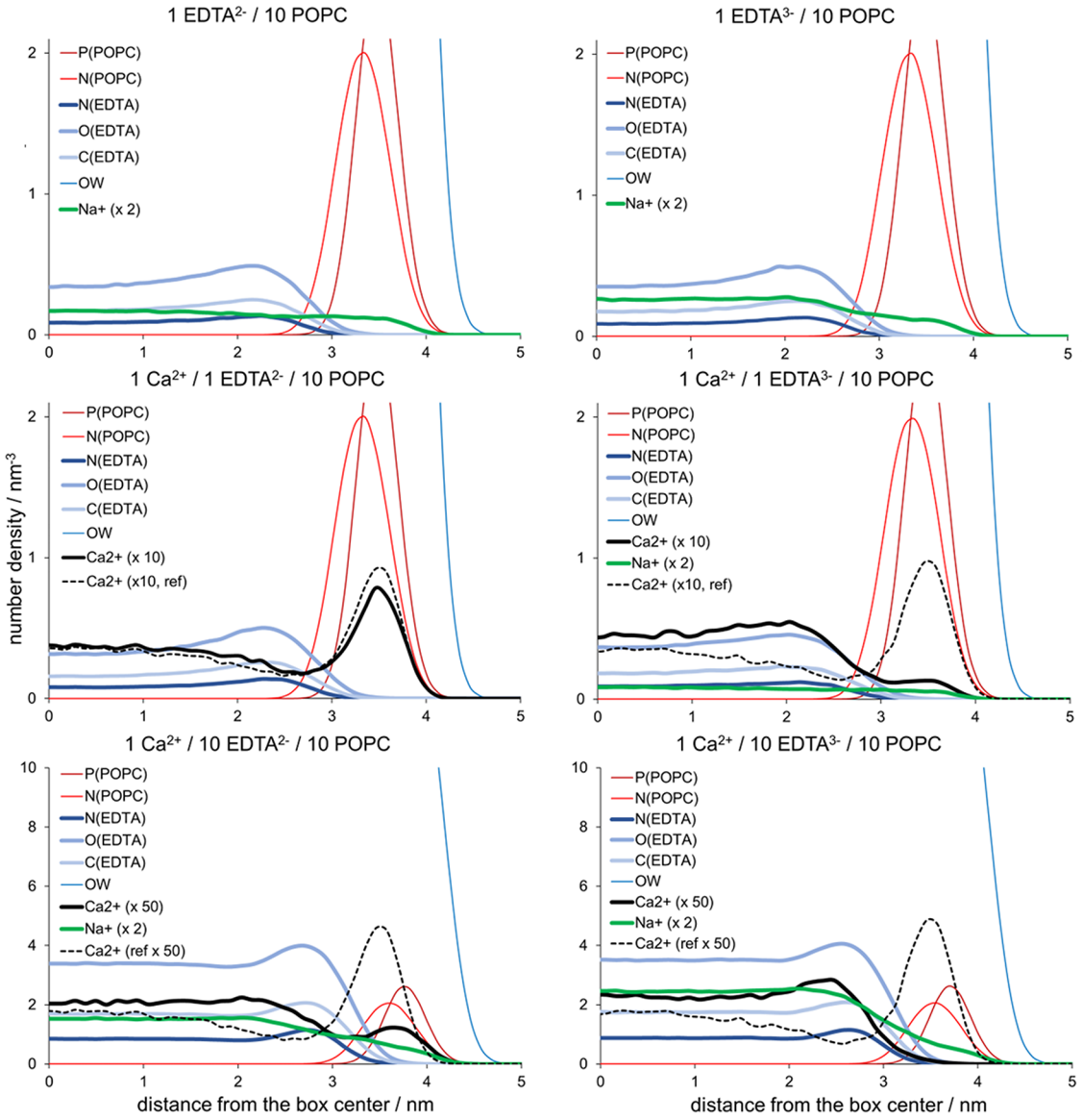

Figure 2. Number density profiles for monolayer phosphate atoms P(POPC), choline nitrogen atoms N(POPC), all nitrogen (N(EDTA)), carboxyl oxygen (O(EDTA)), and carboxyl carbon atoms of EDTA (C(EDTA)), Na^+ and Ca^{2+} cations, and water oxygen atoms (OW) from MD simulations with different ratios of EDTA/Ca^{2+}/POPC. The number density profiles for EDTA atoms and cations are shown in thick lines. The number density of calcium is scaled up by a factor of 10 or 50 (depending on the EDTA concentration) to highlight the effect of its sequestration. Similarly, the number density of sodium is scaled up by a factor of 2. The reference number density profile for Ca^{2+} from EDTA-free systems is shown in a dashed line.

then for 5 min covered with the acrylic box to enable the temperature to equilibrate.

150 mM solution of EDTA was prepared by dissolution of solid EDTA (Sigma-Aldrich; St. Louis, MO) and NaOH (Sigma-Aldrich; St. Louis, MO) in Milli-Q water, and the final pH was set to 8.00 by slow addition of 10 M NaOH solution. 15 mM, 3 mM, 1 mM, 50 μM, and 50 nM EDTA solutions were prepared by dilution of the starting 150 mM solution of EDTA with Milli-Q water, and the pH of the solution was measured before each measurement.

RESULTS AND DISCUSSION

First, we performed molecular dynamics (MD) simulations of 1-palmitoyl-2-oleoylphosphatidylcholine (POPC) monolayers interacting with $EDTA^{2-}$ and $EDTA^{3-}$ anions at different EDTA/Ca^{2+}/POPC ratios (exact composition of the systems is presented in Table S1), and the results are presented in Figure 2. Note that we examine the adsorption of EDTA in two possible protonation states according to corresponding pK_a values and pH (see Figure 1). The analysis of number density profiles in 1 $EDTA^{2-}$/10 POPC and 1 $EDTA^{3-}$/10 POPC systems (upper left and right panels, respectively) shows that despite the high negative charge of EDTA anions, both $EDTA^{2-}$ and $EDTA^{3-}$ have slightly pronounced adsorption peaks at around 1 nm from phosphate POPC atoms. This weak adsorption is present for both EDTA anions and comparable in strength (if not even stronger) to adsorption of only singly negatively charged ions such as Cl^-.[39] Interestingly, the difference in charge between $EDTA^{2-}$ and $EDTA^{3-}$ does not contribute to the strength of adsorption, because negatively charged carboxyl groups of both EDTA anions similarly interact with positively charged POPC choline groups (see

https://doi.org/10.1021/acs.jpcb.3c03207
J. Phys. Chem. B 2023, 127, 5462−5469

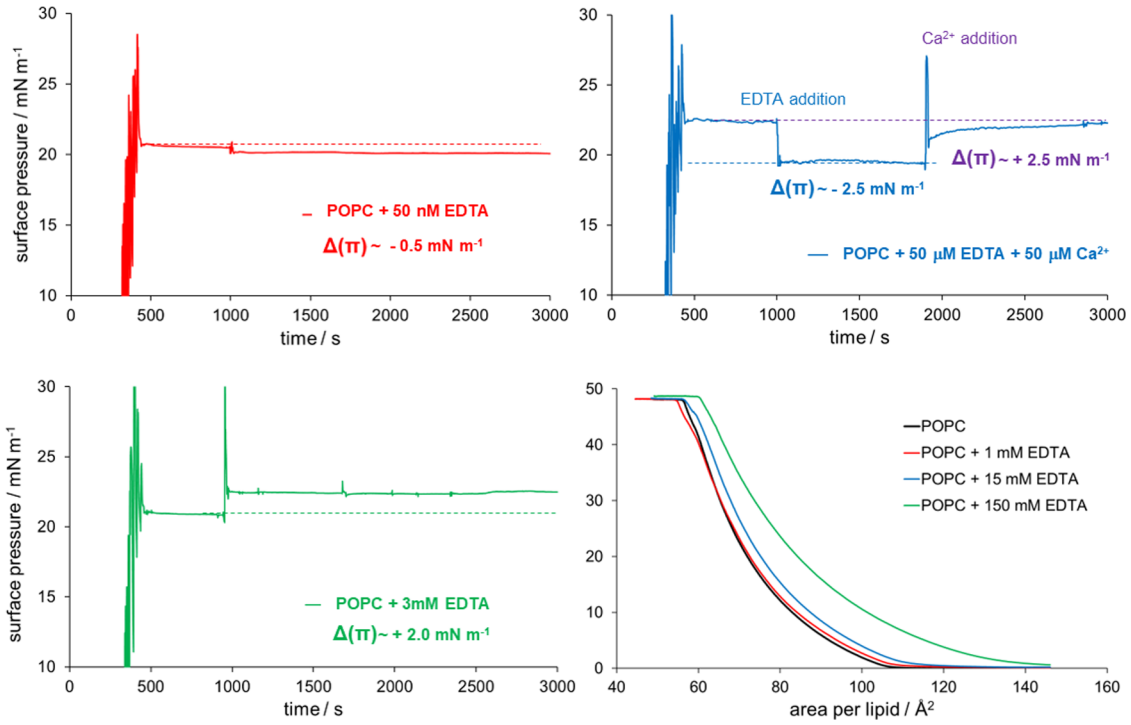

Figure 3. Time dependence of POPC monolayer surface pressure before and after the addition of EDTA (top left and bottom left panel) and EDTA with the subsequent addition of $CaCl_2$ (top right panel). The EDTA concentrations in the solution are 50 nM at pH = 5.5 (red, top left panel), 50 μM at pH = 6.4 (blue, top right panel), and 3 mM at pH = 8 (green, bottom left panel). Langmuir compression isotherms of POPC in the presence of EDTA at different concentrations (multicolor, bottom right panel).

radial distribution functions (RDFs), Figure S3). Specifically, we see two noticeable peaks in the RDFs between the nitrogen atom of POPC choline groups and any carboxyl oxygen atom in both $EDTA^{2-}$ and $EDTA^{3-}$ anions. The first peak is smaller in amplitude and located at ~0.7 nm, whereas a more enhanced peak is located at around ~0.9 nm and corresponds to the maximum density peak of O(EDTA) atoms shown in the number density profiles (Figure 2). Taking this into account, we conclude that the weak interaction between EDTA and POPC choline groups is mainly electrostatic in nature.

The density profile of Na^+ counterions (green color) shows only a small amount close to the membrane surface. However, note that a recent study combining MD simulations, vibrational sum frequency generation, and Langmuir-trough experiments has shown that the presence of Na^+ cations at DPPC monolayers does not disturb the membrane even at high mM concentrations,[40] implying that any changes in the monolayer structure are not induced by sodium and should be attributed to other ions and solutes present in the solution.

In the 1 Ca^{2+}/1 $EDTA^{2-}$/10 POPC system (middle left panel, Figure 2), which is set up to mimic the experiments at low nM EDTA concentrations at pH around 5.5 (Figure 1), we observe that in addition to adsorption of $EDTA^{2-}$, which exhibits an almost identical adsorption pattern as in the reference system (left upper panel), Ca^{2+} ions are still relatively abundant at the POPC monolayer. This observation is evidenced by a higher number density of Ca^{2+} in the headgroup region vs bulk Ca^{2+} concentration in our MD simulations but still in a smaller amount than in EDTA-free simulations containing only Ca^{2+} ions (dashed lines). Therefore, MD simulations indicate only a partial sequestration of Ca^{2+}. Upon extra addition of $EDTA^{2-}$ to the system (1 Ca^{2+}/10 $EDTA^{2-}$/10 POPC, bottom left panel), the number density of Ca^{2+} shows its further removal from the monolayer surface. However, we should note that such an $EDTA^{2-}$-to-calcium ratio is not experimentally observed since adding EDTA increases the pH and, as a result, also increases the $EDTA^{3-}$ concentration at the expense of $EDTA^{2-}$ anions (Figure 1).

Therefore, we also modeled $EDTA^{3-}$-containing systems that more closely correspond to the experiments with higher EDTA concentrations where the pH is around 6.4 (Figure 1). The overall adsorption of $EDTA^{3-}$ is similar in 1 Ca^{2+}/1 $EDTA^{3-}$/10 POPC vs 1 Ca^{2+}/1 $EDTA^{2-}$/10 POPC (Figure 2, middle panels), with one important exception—the sequestration of Ca^{2+} is more efficient in the $EDTA^{3-}$ system compared to analogous $EDTA^{2-}$ and reference EDTA-free systems. Finally, in 1 Ca^{2+}/10 $EDTA^{3-}$/10 POPC system, the sequestration of Ca^{2+} from the monolayer is complete (Figure 2, bottom right panel), indicating more efficient Ca^{2+} depletion with increasing $EDTA^{3-}$ concentration, which is intuitively expected due to the stronger electrostatic Ca^{2+}–$EDTA^{3-}$ interaction vs Ca^{2+}–$EDTA^{2-}$ interaction. Altogether, our conclusions drawn from MD simulations perfectly resemble the anticipated function of EDTA, yet indicating that in all cases, some amount of EDTA remains bound to the lipid monolayer.

For the first experimental measurements, we decided to check the effect of low 50 nm EDTA concentrations at pH = 5.5, where the concentration of EDTA is comparable to the Ca^{2+} concentration in Milli-Q water (used in our experiments) as modeled in the 1 Ca^{2+}/1 $EDTA^{2-}$/10 POPC system.

Using a custom-made microwell with the possibility of substance injection into the subphase and equipped with a surface tensiometer (see the Methods Section for details), we measured how the addition of 50 nM of EDTA affects the surface pressure of the POPC monolayer. We observed only a

https://doi.org/10.1021/acs.jpcb.3c03207
J. Phys. Chem. B 2023, 127, 5462−5469

slight decrease in the surface pressure with time; the POPC monolayer stabilized with surface pressure ca. 0.5 mN m^{-1} lower than before the EDTA addition (Figure 3, top left panel). The drop of pressure is attributed to only a partial removal of Ca^{2+} from the monolayer headgroup region in agreement with a minor decrease in the number density of Ca^{2+} in the 1 Ca^{2+}/1 $EDTA^{2-}$/10 POPC system vs reference EDTA-free system (Figure 2, left middle panel).

Since the removal of Ca^{2+} is incomplete under these experimental conditions, we performed additional experiments at 50 μM EDTA concentration, where the measured pH is 6.4. At this EDTA concentration, the amount of $EDTA^{3-}$ increased vs $EDTA^{2-}$, now them being roughly in the same amount in the solution (Figure 1). An observed drop of the surface pressure after EDTA addition significantly increased from ca. 0.5 to 2.5 mN m^{-1}, which agrees with 1 Ca^{2+}/1 $EDTA^{3-}$/10 POPC and 1 Ca^{2+}/10 $EDTA^{3-}$/10 POPC density profiles (Figure 2, middle and bottom right panels), indicating that Ca^{2+} is more efficiently removed from the POPC surface by $EDTA^{3-}$, especially in the case of the 1 Ca^{2+}/10 $EDTA^{3-}$/10 POPC system where Ca^{2+} is completely depleted from the lipid monolayer (Figure 2, bottom right panel). Moreover, the subsequent addition of 50 μM Ca^{2+} (by corresponding addition of $CaCl_2$ in the subphase) to the same experimental system showed an increase in surface pressure back to the level before the addition of EDTA (Figure 3, top right panel), thus again confirming that EDTA indeed removes Ca^{2+} from the membrane. Finally, we performed adsorption kinetics measurements at 3 mM EDTA concentrations (where pH is slightly larger than 8), which show the increase of surface pressure upon EDTA addition by ca. 2 mN m^{-1} (Figure 3, left bottom panel) due to the elevated effect of EDTA adsorption at higher concentrations, which cancels the effect of Ca^{2+} removal. These results are also confirmed by the independent experiments with different monolayer surface pressure sensors shown in Figure S4.

The Langmuir compression isotherms of POPC monolayers were measured on subphases of Milli-Q water (used as a reference) at 1 mM, 15 mM, and 150 mM of EDTA (see Figure 3, bottom right panel). The measured experimental pH values are slightly larger than 8, indicating that $EDTA^{3-}$ anions are dominantly present in the solution (Figure 1). The interaction of $EDTA^{3-}$ anions with the POPC monolayer is visible at 15 mM and 150 mM EDTA concentrations. The isotherms are shifted horizontally (for area per lipid) and vertically (for surface pressure), and the effect increases with the concentration of added EDTA. The collected isotherms indicate that EDTA interacts and accumulates at the POPC monolayer, thereby increasing the surface pressure for the whole range of areas per lipid. Interestingly, for all EDTA concentrations, the measured isotherms coincide with the isotherm of Milli-Q water in the region of monolayer collapse at low area per lipid values (around 60 $Å^2$), suggesting that a certain amount of EDTA remains trapped in the POPC monolayer until monolayer breakup.

Since the concentration of Ca^{2+} in Langmuir-trough experiments is by many orders of magnitude smaller than concentrations of $EDTA^{3-}$ anions (nM and mM range, respectively), the best comparison with the MD simulation results can be made for Ca^{2+}-free systems, in particular for the 1 $EDTA^{3-}$/10 POPC system where $EDTA^{3-}$ anions are most abundant species at experimental pH = 8. As indicated in our MD results, the adsorption of $EDTA^{3-}$ anions at the POPC monolayer is observed for these conditions (Figure 2, upper right panel). At 1 mM concentration of EDTA, the isotherm is very similar to the referent POPC, and it is not completely clear whether 1 mM EDTA indeed leads to the observed shift in the isotherm and subsequent increase of surface pressure. However, we showed in adsorption kinetics measurements that at lower EDTA concentrations (50 nm and 50 μM), the surface pressure decreases due to at least partial Ca^{2+} sequestration from the membrane, whereas adding 3 mM EDTA leads in contrast to an increase in the surface pressure. Therefore, at the EDTA concentration of 1 mM, which shows only a small difference compared to the measurements on pure POPC, it is fair to assume that the opposite directions of the corresponding trends result in minimal (if any) changes in the surface pressure (Figure 3). In any case, we should stress that EDTA is still adsorbed at the POPC monolayer as shown in the MD simulations even with lower EDTA content (Figure 2).

From the MD simulation data and experimental surface pressure monolayer experiments, we can conclude the following. First, using MD simulations, we demonstrated that calcium sequestration is induced by both $EDTA^{2-}$ and $EDTA^{3-}$ anions already at low EDTA concentrations (Figure 2), which agrees with the experimental adsorption kinetics measurements. However, the fact that the Ca^{2+} sequestration at 50 nM and pH = 5.5 is only partial (Figure 2) suggests that higher concentrations of EDTA should be used for its complete removal. Indeed, in systems with higher EDTA concentrations of 50 μM (corresponding to pH = 6.4, where a more significant amount of $EDTA^{3-}$ is present in solution), MD simulations and experiments predict a more efficient removal of Ca^{2+} from the membrane (Figures 2 and 3). Moreover, the increase of EDTA concentration to 3 mM in adsorption kinetics measurements shows the increase of surface pressure induced by EDTA adsorption. Therefore, using 0.1 mM (or higher) EDTA concentrations in typical biophysical experiments is justified for successful Ca^{2+} removal from the lipid membranes.

Second, and far more intriguingly, we see that in MD simulations, both $EDTA^{2-}$ and $EDTA^{3-}$ anions adsorb to the POPC monolayer at all investigated EDTA concentrations, including the reference system without Ca^{2+}. This observation is supported by a large surface pressure increase in kinetic and isotherm experimental measurements with high mM EDTA concentrations (Figure 3, bottom panels), in agreement with the increased number density of EDTA anions in corresponding MD simulations (Figure 2). These findings imply an additional electrostatic effect of EDTA weakly bound to the membrane. To check for that effect, we calculated the total electrostatic potential of the reference 1 Ca^{2+}/10 POPC system without EDTA and compared it with the 1 Ca^{2+}/10 $EDTA^{2-}$/10 POPC system (Figure 4).

We see that in the EDTA-containing system, a small minimum of ca. 50 mV appears at around 3.5 nm away from the box center (red line), i.e., at the position of the number density profiles maxima of EDTA atom groups (Figure 2). This observation implies that the interaction of other positively charged species with the membrane might be partially screened by negatively charged EDTA, thus inhibiting the interaction with the POPC headgroups themselves.

https://doi.org/10.1021/acs.jpcb.3c03207
J. Phys. Chem. B 2023, 127, 5462−5469

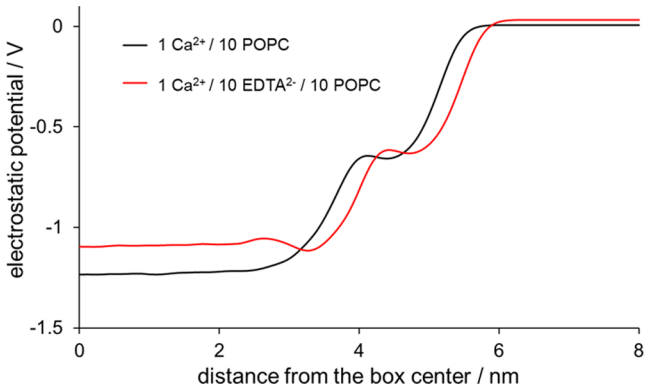

Figure 4. Electrostatic potential of the reference 1 Ca^{2+}/10 POPC (black line) and 1 Ca^{2+}/10 $EDTA^{2-}$/10 POPC systems.

CONCLUSIONS

In conclusion, we presented that the addition of EDTA in 0.1 mM concentrations is justified in biophysical and biological experiments since lower concentrations of EDTA do not lead to complete Ca^{2+} removal from the lipid membranes, as confirmed by both MD simulations and adsorption kinetics measurements. However, with the observed sequestration effect, an additional stealthy action of EDTA is also detected—its adsorption to POPC monolayers at all investigated EDTA concentrations. This behavior is evident from MD simulations but especially in kinetic and isotherm measurements showing an increase of surface pressure at the POPC monolayer with mM concentrations of EDTA. Moreover, given corresponding charge-screening effects induced by EDTA, its adsorption may influence the binding of other positively charged species (such as positively charged cell-penetrating peptides)[41,42] especially when they are present in similarly low mM concentrations like 0.1 mM EDTA often used in biophysical experiments. One of the prominent examples where EDTA action might play a critical role is found in the lack of the translocation of polyarginine cell-penetrating peptides across large POPC unilamellar vesicles (LUVs) in EDTA-containing experiments[24] vs their facile penetration across giant unilamellar POPC vesicles (GUVs) in EDTA-free systems.[43,44] Moreover, the energetics of peptides binding to POPC, known to be dependent also on the ionic strength of the solution,[45] could change significantly when EDTA is present in the system, and the results of experiments involving EDTA should be taken with great care.

ASSOCIATED CONTENT

Data Availability Statement

The data that support the findings of this study are available from the corresponding author upon reasonable request.

Supporting Information

The Supporting Information is available free of charge at https://pubs.acs.org/doi/10.1021/acs.jpcb.3c03207.

Composition of studied systems in MD simulations, atomic types and partial charges of $EDTA^{2-}$ and $EDTA^{3-}$ anions, example snapshot from EDTA-containing MD simulations, RDFs of selected systems, kinetics of POPC monolayer surface pressure changes, simulation model of EDTA anions, and Gromacs topologies for EDTA anions (PDF)

EDTA force fields (ZIP)

AUTHOR INFORMATION

Corresponding Authors

Lukasz Cwiklik − *J. Heyrovský Institute of Physical Chemistry, Czech Academy of Sciences, 18223 Prague, Czech Republic; Institute of Organic Chemistry and Biochemistry of the Czech Academy of Sciences, 16000 Prague, Czech Republic;* orcid.org/0000-0002-2083-8738; Email: lukasz.cwiklik@jh-inst.cas.cz

Mario Vazdar − *Department of Mathematics, Informatics and Cybernetics, University of Chemistry and Technology, 16628 Prague, Czech Republic;* orcid.org/0000-0001-6905-6174; Email: mario.vazdar@vscht.cz

Authors

Katarina Vazdar − *J. Heyrovský Institute of Physical Chemistry, Czech Academy of Sciences, 18223 Prague, Czech Republic;* orcid.org/0000-0003-4952-7965

Carmelo Tempra − *Institute of Organic Chemistry and Biochemistry of the Czech Academy of Sciences, 16000 Prague, Czech Republic;* orcid.org/0000-0002-2890-6993

Agnieszka Olżyńska − *J. Heyrovský Institute of Physical Chemistry, Czech Academy of Sciences, 18223 Prague, Czech Republic;* orcid.org/0000-0001-6533-5280

Denys Biriukov − *Institute of Organic Chemistry and Biochemistry of the Czech Academy of Sciences, 16000 Prague, Czech Republic; Central European Institute of Technology, Masaryk University, 625 00 Brno, Czech Republic;* orcid.org/0000-0003-1007-2203

Complete contact information is available at: https://pubs.acs.org/10.1021/acs.jpcb.3c03207

Author Contributions

⊥K.V. and C.T. contributed equally to this work. K.V., L.C., and M.V. conceptualized the study. C.T. and D.B. performed molecular dynamics simulations, whereas K.V. and A.O. performed the experimental part of the work. All authors interpreted the data and prepared the figures, and M.V. wrote the first version of the manuscript. All authors revised and agreed on its final version.

Notes

The authors declare no competing financial interest.

ACKNOWLEDGMENTS

This work was supported by the Czech Science Foundation (Grant No. 21-19854S) and the project "National Institute of Virology and Bacteriology (Program EXCELES, ID Project No. LX22NPO5103)—Funded by the European Union—Next Generation EU".

REFERENCES

(1) Dwyer, F. *Chelating Agents and Metal Chelates*; Academic Press, 1964; pp 335−382.

(2) Carr, M. H.; Frank, H. A. Improved Method for Determination of Calcium and Magnesium of Biologic Fluids by EDTA Titration. *Am. J. Clin. Pathol.* **1956**, *26*, 1157−1168.

(3) Hart, J. R. Ethylenediaminetetraacetic Acid and Related Chelating Agents. In *Ullmann's Encyclopedia of Industrial Chemistry*; Wiley-VCH Verlag GmbH & Co. KGaA: Weinheim, Germany, 2011; pp 573−578.

(4) Jones, S. S.; Long, F. A. Complex Ions from Iron and Ethylenediaminetetraacetate: General Properties and Radioactive Exchange. *J. Phys. Chem. A* **1952**, *56*, 25−33.

(5) Faust, B. C.; Zepp, R. G. Photochemistry of Aqueous Iron(III)-Polycarboxylate Complexes: Roles in the Chemistry of Atmospheric and Surface Waters. *Environ. Sci. Technol.* **1993**, *27*, 2517−2522.
(6) George, T.; Brady, M. F. Ethylenediaminetetraacetic Acid (EDTA). *Cold Spring Harb Protoc.* **2022**, *2009*, No. pdb.caut2770.
(7) Foreman, M. M.; Weber, J. M. Ion Binding Site Structure and the Role of Water in Alkaline Earth EDTA Complexes. *J. Phys. Chem. Lett.* **2022**, *13*, 8558−8563.
(8) Sillanpää, M.; Oikari, A. Assessing the Impact of Complexation by EDTA and DTPA on Heavy Metal Toxicity Using Microtox Bioassay. *Chemosphere* **1996**, *32*, 1485−1497.
(9) Thompson, K. A.; Goodale, D. B. The Recent Development of Propofol (DIPRIVAN). *Intensive Care Med.* **2000**, *26*, S400−S404.
(10) Ittoop, S. M.; Seibold, L. K.; Kahook, M. Y.Ocular Surface Disease and the Role of Preservatives in Glaucoma Medications. In *Glaucoma*; Elsevier, 2015; Vol. *1*, pp 593−597.
(11) Wreesmann, C. T. J. Reasons for Raising the Maximum Acceptable Daily Intake of EDTA and the Benefits for Iron Fortification of Foods for Children 6−24 Months of Age. *Matern. Child Nutr.* **2014**, *10*, 481−495.
(12) Lanigan, R. S.; Yamarik, T. A.; Andersen, F. A. Final Report on the Safety Assessment of EDTA, Calcium Disodium EDTA, Diammonium EDTA, Dipotassium EDTA, Disodium EDTA, TEA-EDTA, Tetrasodium EDTA, Tripotassium EDTA, Trisodium EDTA, HEDTA, and Trisodium HEDTA. *Int. J. Toxicol.* **2016**, *21*, 95−142.
(13) Haque, H.; Russell, A. D. Effect of Ethylenediaminetetraacetic Acid and Related Chelating Agents on Whole Cells of Gram-Negative Bacteria. *Antimicrob. Agents Chemother.* **1974**, *5*, 447−452.
(14) Alakomi, H. L.; Saarela, M.; Helander, I. M. Effect of EDTA on Salmonella Enterica Serovar Typhimurium Involves a Component Not Assignable to Lipopolysaccharide Release. *Microbiology* **2003**, *149*, 2015−2021.
(15) EDTA | Blade Wiki | Fandom. EDTA is Used as a Weapon to Kill Vampires, 2023. https://blade.fandom.com/wiki/EDTA. (accessed March 07, 2023).
(16) Sorour, M. H.; Hani, H. A.; Shaalan, H. F.; El-Sayed, M. M. H. Experimental Screening of Some Chelating Agents for Calcium and Magnesium Removal from Saline Solutions. *Desalin. Water Treat.* **2016**, *57*, 22799−22808.
(17) Rahman, Y. E.; Wright, B. J. Liposomes Containing Chelating Agents. Cellular Penetration and a Possible Mechanism of Metal Removal. *J. Cell Biol.* **1975**, *65*, 112−122.
(18) Dominguez, K.; Ward, W. S. A Novel Nuclease Activity That Is Activated by Ca2+ Chelated to EGTA. *Syst. Biol. Reprod. Med.* **2009**, *55*, 193−199.
(19) Napirei, M.; Wulf, S.; Eulitz, D.; Mannherz, H. G.; Kloeckl, T. Comparative Characterization of Rat Deoxyribonuclease 1 (Dnase1) and Murine Deoxyribonuclease 1-like 3 (Dnase1l3). *Biochem. J.* **2005**, *389*, 355−364.
(20) Meyboom, A.; Maretzki, D.; Stevens, P. A.; Hofmann, K. P. Reversible Calcium-Dependent Interaction of Liposomes with Pulmonary Surfactant Protein A. *J. Biol. Chem.* **1997**, *272*, 14600−14605.
(21) Kikuchi, T.; Suzuki, M.; Kusai, A.; Iseki, K.; Sasaki, H. Synergistic Effect of EDTA and Boric Acid on Corneal Penetration of CS-088. *Int. J. Pharm.* **2005**, *290*, 83−89.
(22) Prachayasittikul, V.; Isarankura-Na-Ayudhya, C.; Tantimongcolwat, T.; Nantasenamat, C.; Galla, H. J. EDTA-Induced Membrane Fluidization and Destabilization: Biophysical Studies on Artificial Lipid Membranes. *Acta Biochim. Biophys. Sin.* **2007**, *39*, 901−913.
(23) Melcrová, A.; Pokorna, S.; Pullanchery, S.; Kohagen, M.; Jurkiewicz, P.; Hof, M.; Jungwirth, P.; Cremer, P. S.; Cwiklik, L. The Complex Nature of Calcium Cation Interactions with Phospholipid Bilayers. *Sci. Rep.* **2016**, *6*, No. 38035.
(24) Allolio, C.; Magarkar, A.; Jurkiewicz, P.; Baxová, K.; Javanainen, M.; Mason, P. E.; Šachl, R.; Cebecauer, M.; Hof, M.; Horinek, D.; et al. Arginine-Rich Cell-Penetrating Peptides Induce Membrane Multilamellarity and Subsequently Enter via Formation of a Fusion Pore. *Proc. Natl. Acad. Sci. U.S.A.* **2018**, *115*, 11923−11928.
(25) Rupprecht, A.; Sokolenko, E. A.; Beck, V.; Ninnemann, O.; Jaburek, M.; Trimbuch, T.; Klishin, S. S.; Jezek, P.; Skulachev, V. P.; Pohl, E. E. Role of the Transmembrane Potential in the Membrane Proton Leak. *Biophys. J.* **2010**, *98*, 1503−1511.
(26) Stangherlin, A.; Watson, J. L.; Wong, D. C. S.; Barbiero, S.; Zeng, A.; Seinkmane, E.; Chew, S. P.; Beale, A. D.; Hayter, E. A.; Guna, A.; et al. Compensatory Ion Transport Buffers Daily Protein Rhythms to Regulate Osmotic Balance and Cellular Physiology. *Nat. Commun.* **2021**, *12*, No. 6035.
(27) Berg, J. M.; Tymoczko, J. L.; Stryer, L. *Biochemistry*, 5th ed.; Berg, J. M.; Tymoczko, J. L.; Stryer, L., Eds.; W.H. Freeman: New York NY, 2002; pp 84−137.
(28) Javanainen, M.; Lamberg, A.; Cwiklik, L.; Vattulainen, I.; Ollila, O. H. S. Atomistic Model for Nearly Quantitative Simulations of Langmuir Monolayers. *Langmuir* **2018**, *34*, 2565−2572.
(29) Klauda, J. B.; Venable, R. M.; Freites, J. A.; O'Connor, J. W.; Tobias, D. J.; Mondragon-Ramirez, C.; Vorobyov, I.; MacKerell, A. D.; Pastor, R. W. Update of the CHARMM All-Atom Additive Force Field for Lipids: Validation on Six Lipid Types. *J. Phys. Chem. B* **2010**, *114*, 7830−7843.
(30) Izadi, S.; Anandakrishnan, R.; Onufriev, A. V. Building Water Models: A Different Approach. *J. Phys. Chem. Lett.* **2014**, *5*, 3863−3871.
(31) Tempra, C.; Ollila, O. H. S.; Javanainen, M. Accurate Simulations of Lipid Monolayers Require a Water Model with Correct Surface Tension. *J. Chem. Theory Comput.* **2022**, *18*, 1862−1869.
(32) Kim, S.; Lee, J.; Jo, S.; Brooks, C. L.; Lee, H. S.; Im, W. CHARMM-GUI Ligand Reader and Modeler for CHARMM Force Field Generation of Small Molecules. *J. Comput. Chem.* **2017**, *38*, 1879−1886.
(33) Lee, J.; Cheng, X.; Swails, J. M.; Yeom, M. S.; Eastman, P. K.; Lemkul, J. A.; Wei, S.; Buckner, J.; Jeong, J. C.; Qi, Y.; et al. CHARMM-GUI Input Generator for NAMD, GROMACS, AMBER, OpenMM, and CHARMM/OpenMM Simulations Using the CHARMM36 Additive Force Field. *J. Chem. Theory Comput.* **2016**, *12*, 405−413.
(34) Vanommeslaeghe, K.; Raman, E. P.; MacKerell, A. D. Automation of the CHARMM General Force Field (CGenFF) II: Assignment of Bonded Parameters and Partial Atomic Charges. *J. Chem. Inf. Model.* **2012**, *52*, 3155−3168.
(35) Essmann, U.; Perera, L.; Berkowitz, M. L.; Darden, T.; Lee, H.; Pedersen, L. G. A Smooth Particle Mesh Ewald Method. *J. Chem. Phys.* **1995**, *103*, 8577−8593.
(36) Shirts, M. R.; Mobley, D. L.; Chodera, J. D.; Pande, V. S. Accurate and Efficient Corrections for Missing Dispersion Interactions in Molecular Simulations. *J. Phys. Chem. B* **2007**, *111*, 13052−13063.
(37) Hess, B. P-LINCS: A Parallel Linear Constraint Solver for Molecular Simulation. *J. Chem. Theory Comput.* **2008**, *4*, 116−122.
(38) Abraham, M. J.; Murtola, T.; Schulz, R.; Páll, S.; Smith, J. C.; Hess, B.; Lindah, E. Gromacs: High Performance Molecular Simulations through Multi-Level Parallelism from Laptops to Supercomputers. *SoftwareX* **2015**, *1−2*, 19−25.
(39) Melcr, J.; Martinez-Seara, H.; Nencini, R.; Kolafa, J.; Jungwirth, P.; Ollila, O. H. S. Accurate Binding of Sodium and Calcium to a POPC Bilayer by Effective Inclusion of Electronic Polarization. *J. Phys. Chem. B* **2018**, *122*, 4546−4557.
(40) Javanainen, M.; Hua, W.; Tichacek, O.; Delcroix, P.; Cwiklik, L.; Allen, H. C. Structural Effects of Cation Binding to DPPC Monolayers. *Langmuir* **2020**, *36*, 15258−15269.
(41) Vazdar, M.; Wernersson, E.; Khabiri, M.; Cwiklik, L.; Jurkiewicz, P.; Hof, M.; Mann, E.; Kolusheva, S.; Jelinek, R.; Jungwirth, P. Aggregation of Oligoarginines at Phospholipid Membranes: Molecular Dynamics Simulations, Time-Dependent Fluorescence Shift, and Biomimetic Colorimetric Assays. *J. Phys. Chem. B* **2013**, *117*, 11530−11540.

https://doi.org/10.1021/acs.jpcb.3c03207
J. Phys. Chem. B 2023, 127, 5462−5469

(42) Robison, A. D.; Sun, S.; Poyton, M. F.; Johnson, G. A.; Pellois, J. P.; Jungwirth, P.; Vazdar, M.; Cremer, P. S. Polyarginine Interacts More Strongly and Cooperatively than Polylysine with Phospholipid Bilayers. *J. Phys. Chem. B* **2016**, *120*, 9287−9296.
(43) Sakamoto, K.; Morishita, T.; Aburai, K.; Ito, D.; Imura, T.; Sakai, K.; Abe, M.; Nakase, I.; Futaki, S.; Sakai, H. Direct Entry of Cell-Penetrating Peptide Can Be Controlled by Maneuvering the Membrane Curvature. *Sci. Rep.* **2021**, *11*, No. 31.
(44) Sakamoto, K.; Kitano, T.; Kuwahara, H.; Tedani, M.; Aburai, K.; Futaki, S.; Abe, M.; Sakai, H.; Ohtaka, H.; Yamashita, Y. Effect of Vesicle Size on the Cytolysis of Cell-Penetrating Peptides (CPPs. *Int. J. Mol. Sci.* **2020**, *21*, No. 7405.
(45) Nguyen, M. T. H.; Biriukov, D.; Tempra, C.; Baxova, K.; Martinez-Seara, H.; Evci, H.; Singh, V.; Šachl, R.; Hof, M.; Jungwirth, P.; et al. Ionic Strength and Solution Composition Dictate the Adsorption of Cell-Penetrating Peptides onto Phosphatidylcholine Membranes. *Langmuir* **2022**, *38*, 11284−11295.

https://doi.org/10.1021/acs.jpcb.3c03207
J. Phys. Chem. B 2023, 127, 5462−5469